A continuous-time LPV models for a biofiltration process in wastewater nitrification - A global approach methodology for parametric estimation

Fatima Zahra Boutourda, Régis Ouvrard, Thierry Poinot, Driss Mehdi, Fouad Mesquine, Éloïse de Tredern, Vincent Jauzein

A continuous-time LPV models for a biofiltration process in wastewater nitrification - A global approach methodology for parametric estimation

Fatima Zahra Boutourda[a,b,*], Régis Ouvrard[a], Thierry Poinot[a], Driss Mehdi[a], Fouad Mesquine[b], Éloïse De Tredern[c], Vincent Jauzein[c]

[a] *Université de Poitiers, ISAE-ENSMA, LIAS, 2 rue Pierre Brousse, TSA 41105, 86073 Poitiers cedex 9 France. (e-mail: regis.ouvrard@univ-poitiers.fr)*
[b] *Université Cadi Ayyad, Faculté des Sciences Semlalia, EA2(SI), Marrakech Maroc.*
[c] *Syndicat interdépartemental pour l'assainissement de l'agglomération parisienne, 82 avenue Kléber, 92700 Colombes France.*

Abstract

Biological wastewater treatment processes are essential in the sustainable management of water resources, offering an efficient method for removing contaminants and pollutants, such as ammonium, from wastewater to protect both public health and the environment. Among various treatment methods, submerged aerated biofilters stand out for their efficiency in converting high ammonium concentrations into nitrate. This process stimulates the growth of specific microorganisms on filtering materials, aiding in efficient pollutant conversion.

However, the complexity of biological wastewater treatment processes presents significant modeling challenges, especially under varying operational conditions. Linear Parameter-Varying (LPV) models have emerged as a promising solution to accurately represent these nonlinear systems. Despite their potential, constructing LPV models remains complex, especially for intricate biological treatment processes like wastewater treatment.

This paper presents a novel methodology within the global approach framework for estimating continuous-time LPV models. The proposed approach addresses the challenge of initializing iterative procedures due to the lack of prior knowledge about LPV model parameters. By extending the reinitialized partial moment approach to LPV models, the methodology provides an effective pre-estimate for initializing parameter estimation algorithms. Validation of the proposed methodology through simulation examples establishes a robust foundation for extending the approach to real-world applications, such as estimating LPV models for the nitrification process in wastewater treatment plants.

Keywords: Biofiltration, global approach estimation, instrumental variable, LPV models, nitrification, output-error algorithm, reinitialized partial moment, wastewater treatment

1. Introduction

In nitrification processes, biological wastewater treatment plants need to run continuously to meet strict environmental regulations and deal with varying flows and pollutant concentrations. One of the goals of these processes is to reduce ammonium levels in treated water. A good solution for this is using submerged aerated biofilters. A key advantage of this technology is the high yield/footprint ratio. This process allows the efficient conversion of high fluxes of ammonium into nitrate thanks to microbial metabolism and growth on the filtering media (Payraudeau et al., 2000; Canler et al., 2003). Implementing such methods not only ensures compliance with regulations but also promotes sustainable water management, which is crucial for protecting the environment.

Nitrification processes can be designed by using dynamic mathematical models. Considering the strong nonlinearity of these processes, linear parameter-varying (LPV) models are a promising option. LPV models, characterized by dynamics that vary with the operating point (Lee and Poolla, 1999; Verdult and Verhaegen, 2005; Toth, 2008; Laurain et al., 2010), offer high precision in approximating nonlinear systems with lower order compared to linear model approximations. Nonetheless, constructing an LPV model for a specific nonlinear plant remains a significant challenge. The existing LPV identification approaches predominantly operate within discrete-time frameworks, typically assum-

*Corresponding author

ing a dependence only on the instantaneous value of the scheduling variable. These methods are distinguished by the type of LPV model structure employed, such as Input-Output (Bamieh and Giarré (2002); Wei and Del Re (2006); Giarré et al. (2006)), State space (Lee and Poolla (1999); van Wingerden et al. (2007); Felici et al. (2007); Lovera and Mercère (2007)), or models based on orthogonal basis functions (Toth, 2008).

In the literature, two primary approaches are recognized for the identification of LPV models. The first approach is the global approach, which operates on the assumption that a global identification experiment can be conducted, effectively stimulating all nonlinearities of the system while persistently altering the system dynamics through scheduling variable changes (Lee and Poolla, 1999; Bamieh and Giarré, 2002; Verdult and Verhaegen, 2005; Giarré et al., 2006; Felici et al., 2007; van Wingerden et al., 2007; Toth, 2008; Laurain et al., 2010; Chouaba et al., 2011). The second approach, the local approach, relies on interpolating local linear time-invariant models corresponding to fixed operating points of the system, *i.e.* for constant values of the scheduling variables (Steinbuch et al., 2003; Lovera and Mercère, 2007; De Caigny et al., 2009; Mercère et al., 2011).

This paper introduces a methodology within the framework of the global approach for estimating a continuous-time LPV model which is more realistic for the considered nitrification application in terms of experimental measurements. Output-error algorithms serve as efficient tools in this context. However, these iterative procedures, based on nonlinear optimizations, require an initial parameter vector. Given the difficulty to have *a priori* knowledge about parameters in LPV models, initializing these algorithms poses a significant challenge. Inadequate initialization can result in convergence towards a local optimum or divergence of the optimization algorithm. To address this issue, we propose a novel equation-error estimate, derived from extending the reinitialized partial moment approach to LPV models (Ouvrard and Trigeassou, 2011; Ouvrard et al., 2024), which provides a pre-estimate serving as the initial parameter vector.

The paper is organized as follows. The biofiltration process, the considered application and the LPV framework are presented in Sections 2 and 3. The proposed methodology is described in Section 4 for the parameters estimation. Then, an initial objective is to validate our proposed approach by applying it to a simulation example in Section 5. In this simulation context, the proposed output-error algorithm is compared with an instrumental variable approach. Following this validation step, we intend to apply in Section 6 our methodology to estimate an LPV model for the nitrification process of the Seine Aval wastewater plant, with the perspective of optimizing this process.

2. The biofiltration process

2.1. Plant description

The SIAAP (Syndicat Interdépartemental pour l'Assainissement de l'Agglomération Parisienne (Interdepartmental Syndicate for the Sanitation of Greater Paris)) treats the wastewater of almost 9 million people living in Paris metropolitan area (France), as well as rainwater and water polluted by industry.

The Seine Aval wastewater treatment plant, located in Achères (Yvelines, France), has been studied within the scope of this project. This facility, covering an area of 600 hectares, processes daily 1,500,000 m^3 of wastewater, discharging it into the Seine River. Its water treatment process begins with a pretreatment phase, a physical process aiming at removing the largest materials from the effluent including various units in the installation such as grit removal, degreasing and deoiling. This is followed by a primary treatment phase, which separates suspended solids and floatable materials via sedimentation, consequently reducing chemical/biochemical oxygen demand and phosphate (Rich, 1961). The process continues with a secondary treatment phase, which employs biological methods to eliminate mostly dissolved pollutants such as organic compounds (represented as biological oxygen demand) or ammonium from wastewater post-primary treatment. Processes like activated sludge use suspended bacterial growth, while fixed culture methods, like biofiltration process, utilize surfaces for microbial attachment, enhancing treatment efficiency and low footprint. The following section provides an in-depth explanation of the biofiltration process.

2.2. Biofiltration process

Biofiltration is a fixed-bed culture process that can be employed for secondary biological treatment (Stensel and Reiber, 1983). The biofiltration process is carried out with the biological reactors also known as biofilters (BAF, Biological Aerated Filter or Biological Active Filter). They facilitate both biological treatment and a certain level of liquid-solid separation within a single reactor. A biofilter comprises a column filled with granular filter media colonized by purifying biomasses (Rocher et al., 2008). As wastewater passes through the filter media, organic matter and nutrients are degraded

by the biomasses, while particles are trapped within the media. Typically, the height of filter media (media bed) used in biofilters ranges between 2 and 4 m (Stensel et al., 1988; Pujol et al., 1992). The media, having a diameter between 2 and 5 mm (Metcalf & Eddy et al., 2003), can be fabricated from various materials (clay, pumice, polystyrene, etc.). Based on their density, media can be classified as "heavy" media, which have a density greater than that of water, and floating media, which are less dense than water. This media categorization influences the choice of water feed configuration. A biofilter filled with "heavy" media can be fed with either downward or upward flow, whereas a biofilter using floating media can only operate with upward flow (Mendoza-Espinosa and Stephenson, 1999). Presently, the majority of biofilters are fed with upward flow, allowing them to handle higher influent flow rates (Rocher et al., 2008).

Several companies have developed various technologies of biofilters applied to wastewater treatment. In the Seine Aval wastewater treatment plant, there are 58 pre-denitrifying biofilters, 84 nitrifying biofilters, and 12 post-denitrifying biofilters.

2.3. Nitrification

The nitrification unit studied in this work is divided into three blocks of 28 biofilters (Biostyr), each block comprising two sets of 14 biofilters. Each Biostyr filter has an area of 173 m^2 and is filled with 3.5 m of filtering material. The filter media consists of expanded polystyrene beads with an average diameter of 4 mm (biostyrene).

Nitrification involves the biochemical conversion of ammoniacal nitrogen (NH_4^+) into nitrate (NO_3^-), requiring a sufficient concentration of dissolved oxygen.

This conversion is carried out by two types of autotrophic bacteria: ammonium-oxidizing bacteria (AOB) and nitrite-oxidizing bacteria (NOB). Ammonium-oxidizing bacteria oxidize NH_4^+ as an energy source and utilize CO_2 as a carbon source for their growth. During the metabolism of nitrite-oxidizing bacteria, ammoniacal nitrogen is oxidized to nitrite. Nitrite-oxidizing bacteria further oxidize nitrite to nitrate, using the nitrite produced by ammonium-oxidizing bacteria as an energy source, while also utilizing CO_2 as a carbon source (Henze et al., 2008). The two basic reactions for nitrification are the following (Henze et al., 2008)

$$NH_4^+ + 3/2\ O_2 \rightarrow NO_2^- + H_2O + 2H^+, \quad (1)$$

$$NO_2^- + 1/2\ O_2 \rightarrow NO_3^-. \quad (2)$$

During this process, protons (H^+) are produced, consuming the alkalinity of the medium. This consumption of alkalinity can subsequently impact the nitrification rate, as the process is significantly slowed when the pH of the medium drops below 7 (Metcalf & Eddy et al., 2014). Maintaining an optimal pH is therefore essential to ensure efficient nitrification, as acidic conditions can inhibit the activity of both AOB and NOB communities.

In addition to pH, the availability of dissolved oxygen is another crucial factor affecting nitrification. As nitrifying bacteria are aerobic, they depend on sufficient oxygen levels for energy production and growth. In aerobic biological reactors, these autotrophic nitrifying bacteria must compete with heterotrophic bacteria for available dissolved oxygen. Heterotrophs, which break down organic compounds in the wastewater, often consume oxygen more quickly than autotrophs, creating a competitive environment that can limit nitrification rates, especially under high organic loading conditions (Zhu, 2020).

In the literature, several models, such as the Activated Sludge Model No. 1 (ASM1) (Henze et al., 1987), provide a detailed, mechanistic representation of nitrogen transformations during the nitrification process, making it valuable for biochemical analysis. However, from a control point of view, these mechanistic models are too complex for the synthesis of control laws. We have therefore chosen to use an input-output model capable of capturing the main dynamics and non-linearities. To this end, we have chosen to use an LPV model as described in the next section.

2.4. The input-output considered model

In this paper, we aim to characterize the nitrification process as a continuous-time SISO system, where the air flow rate Q_{air} is designated as the input, while the ammonium concentration at the process output C_{out} serves as the system output.

To effectively control ammonia removal, it is essential to establish a sufficiently accurate model for the nitrification system (Figure 1). Based on various experimental tests, it has been observed that the transfer function C_{out}/Q_{air} is nonlinear and dependent on the operating conditions specified by the water flow rate Q_{water}, the ammonium concentration at the process entrance C_{in} and the air flow rate Q_{air}. Hence, we opt to model the transfer function C_{out}/Q_{air} using an LPV model, with Q_{water}, C_{in} and Q_{air} as scheduling variables. Unlike a mechanistic model, this LPV model is a blackbox structure well-suited to capture the nonlinear dynamics. In this way, the nitrification process is approximated with

a varying linear representation with the operating conditions. In addition to providing an input-output representation of the system over its operating range, these models are widely used in the development of advanced control strategies.

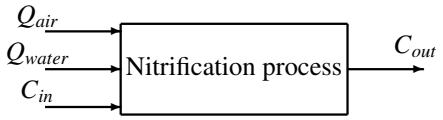

Figure 1: Input-output representation of the nitrification process

3. System and continuous-time LPV model

Toth (2010) proposes various formulations for the discrete-time or continuous-time LPV systems. In this paper, we consider the input-output representation of continuous-time SISO LPV systems with order n_a also described in (Laurain et al., 2011). In such a case, the n_a-th derivative of the true system output $y_0(t)$ can be defined by

$$y_0^{(n_a)}(t) = -\sum_{i=0}^{n_a-1} a_i(\rho) y_0^{(i)}(t) + \sum_{i=0}^{n_b} b_i(\rho) u^{(i)}(t), \quad (3)$$

with $n_a \geq n_b$ and $\rho = \rho(t)$, the scheduling variable bounded to the operating domain. Let us assume that the scheduling variable $\rho(t)$ and its derivatives are known, measurable or computable. The varying parameters $a_i(\rho)$ and $b_i(\rho)$ are assumed to be meromorphic functions[1] of the scheduling variable $\rho(t)$ with no singularity on the considered domain. These parameters are defined with the following structure

$$\begin{aligned} a_i(\rho) &= a_i^0 + \sum_{\ell=1}^{r_f} a_i^\ell f_\ell(\rho), \\ b_i(\rho) &= b_i^0 + \sum_{\ell=1}^{r_g} b_i^\ell g_\ell(\rho). \end{aligned} \quad (4)$$

$f_\ell(\rho)$ and $g_\ell(\rho)$ are assumed to be functions with a static dependence of $\rho(t)$, *i.e.* no derivative of $\rho(t)$. The values of these functions can be calculated directly from $\rho(t)$ or via a mathematical function.

The considered system is assumed to be globally bounded-input/bounded-output stable for all trajectories $\rho(t)$. The signals $u(t)$ and $\rho(t)$ are known at sampled instants with a sampling period Δt, and $y(t)$ is the measurement of the true output $y_0(t)$ with an additive zero-mean disturbance $v(t)$ at the same instants, *i.e.* $y(k\Delta t) = y_0(k\Delta t) + v(k\Delta t)$. The disturbance $v(t)$ is supposed to be uncorrelated with signals $u(t)$ and $\rho(t)$.

[1] A function g is meromorphic if $g = h/q$ where h and q are holomorphic (analytic) functions and q is not null.

4. The methodology for parametric estimation

4.1. Problem statement

By assuming known n_a, n_b, r_f and r_g, the goal is to estimate the constant parameter set

$$\left\{a_i^\ell\right\}_{i=0,\cdots,n_a-1}^{\ell=0,\cdots,r_f}, \ \left\{b_i^\ell\right\}_{i=0,\cdots,n_b}^{\ell=0,\cdots,r_g}, \quad (5)$$

from the data set $\{u(k\Delta t), y(k\Delta t), \rho(k\Delta t)\}_{k=0,\cdots,N_t}$.

Let us define the quadratic criterion

$$J = \frac{1}{N_t+1} \sum_{k=0}^{N_t} \|y(k\Delta t) - \widehat{y}(k\Delta t, \boldsymbol{\theta})\|_2^2, \quad (6)$$

where $\widehat{y}(k\Delta t, \boldsymbol{\theta})$ is the response corresponding to the continuous-time LPV model for the input $u(k\Delta t)$ and the scheduling variable $\rho(k\Delta t)$, with the parameter vector to be identified

$$\begin{aligned} \boldsymbol{\theta} = [&a_0^0, \ldots, a_0^{r_f}, \ldots, a_{n_a-1}^0, \ldots, a_{n_a-1}^{r_f}, \\ &b_0^0, \ldots, b_0^{r_g}, \ldots, b_{n_b}^0, \ldots, b_{n_b}^{r_g}]^\top \end{aligned} \quad (7)$$

of size $N_\theta = n_a\, r_f + (n_b+1)\, r_g$.

4.2. Continuous-time LPV reinitialized partial moment-based model

The main problem with the direct continuous-time system identification is to approximate the unmeasurable input-output derivates, *i.e.* $y_0^{(i)}(t)$ and $u^{(i)}(t)$ with $i > 0$ in (3). Ouvrard and Trigeassou (2011) (see also Ouvrard et al. (2024)) have shown that, by applying integrals and more specifically partial moments to an ordinary differential equation (ODE), it is possible to remove all derivatives and to formulate the ODE output in a linear regression form. Moreover, they prove that the ODE output can be represented by an embedded finite impulse response (FIR) filter models by introducing the n_a-th order reinitialized partial moment filter defined by

$$m_{n_a}(t) = \begin{cases} \dfrac{(\widehat{T}-t)^{n_a} t^{n_a-1}}{(n_a-1)!\widehat{T}^{n_a}}, & \text{for } t \in [0, \widehat{T}], \\ 0 \ \text{ elsewhere}, \end{cases} \quad (8)$$

where $\hat{T}$ is the design parameter called the reinitialization parameter. $\hat{T}$ is the width of the sliding interval

of integration of the partial moments to preserve the minimum variance property of the model at each time t (see Ouvrard and Trigeassou (2011) and Ouvrard et al. (2024) for more details).

The aim of the present section is to extend the reinialized partial moment (RPM) approach and to define the continuous-time LPV RPM-based model. To do this, let us calculate the convolution product $m_{n_a}(t) * (3)$. By considering the property given by

$$\begin{aligned} m_{n_a}^{(i)}(t) * (f_\ell(\rho) y_0(t)) &= m_{n_a}(t) * (f_\ell(\rho) y_0(t))^{(i)} \\ &= m_{n_a}(t) * \sum_{k=0}^{i} \left(\begin{array}{c} i \\ k \end{array} \right) (f_\ell(\rho))^{(i-k)} y_0^{(k)}(t) \end{aligned}, \quad (9)$$

with the binomial coefficients

$$\left(\begin{array}{c} i \\ k \end{array} \right) = \frac{i!}{k!(i-k)!}, \quad (10)$$

and noting that

$$\begin{aligned} m_{n_a}(t) * y_0^{(n_a)}(t) &= m_{n_a}^{(n_a)}(t) * y_0(t) \\ &= y_0(t) - \left(\delta(t) - m_{n_a}^{(n_a)}(t)\right) * y_0(t) \end{aligned}, \quad (11)$$

where $\delta(t)$ is the Dirac function, it is possible to rewrite this convolution product with the following linear regression formulation

$$y_0(t) = \boldsymbol{\varphi}^\top(t)\boldsymbol{\theta} + \left(\delta(t) - m_{n_a}^{(n_a)}(t)\right) * y_0(t), \quad (12)$$

where

$$\boldsymbol{\varphi}(t) = \left[\begin{array}{c} \vdots \\ \displaystyle\sum_{k=0}^{i} (-1)^{k+1} m_{n_a}^{(i-k)}(t) * \left(\begin{array}{c} i \\ k \end{array} \right) \boldsymbol{F}^{(k)}(t) y_0(t) \\ \vdots \\ \displaystyle\sum_{k=0}^{j} (-1)^{k} m_{n_a}^{(j-k)}(t) * \left(\begin{array}{c} j \\ k \end{array} \right) \boldsymbol{G}^{(k)}(t) u(t) \\ \vdots \end{array} \right], \quad (13)$$

with $i = 0 \dots n_a - 1,\ j = 0 \dots n_b$,

$$\boldsymbol{F}(t) = \left[\begin{array}{cccc} 1 & f_1(\rho) & \dots & f_{r_f}(\rho) \end{array} \right]^\top \text{ and}$$
$$\boldsymbol{G}(t) = \left[\begin{array}{cccc} 1 & g_1(\rho) & \dots & g_{r_g}(\rho) \end{array} \right]^\top.$$

The linear regression (12) can be reformulated as follows

$$y_0(t) = \boldsymbol{\varphi}^\top(t)\boldsymbol{\theta} + \gamma^{y_0}(t), \quad (14)$$

where

$$\boldsymbol{\varphi}(t) = \left[\begin{array}{c} \vdots \\ \displaystyle\sum_{k=0}^{i} (-1)^{k} \alpha_{i-k}^{\boldsymbol{z}_k^i}(t) \\ \vdots \\ \displaystyle\sum_{k=0}^{j} (-1)^{k} \beta_{j-k}^{\boldsymbol{w}_k^j}(t) \\ \vdots \end{array} \right], \quad (15)$$

and $\boldsymbol{z}_k^i(t)$ and $\boldsymbol{w}_k^j(t)$ are signal vectors defined by

$$\begin{aligned} \boldsymbol{z}_k^i(t) &= \left(\begin{array}{c} i \\ k \end{array} \right) \boldsymbol{F}^{(k)}(t) y_0(t), \\ \boldsymbol{w}_k^j(t) &= \left(\begin{array}{c} j \\ k \end{array} \right) \boldsymbol{G}^{(k)}(t) u(t), \end{aligned} \quad (16)$$

with $i = 0 \dots n_a - 1,\ j = 0 \dots n_b$,

$$\begin{aligned} \beta_i^g(t) &= m_{n_a}^{(i)}(t) * g(t), \\ \alpha_i^g(t) &= -m_{n_a}^{(i)}(t) * g(t), \\ \gamma^{y_0}(t) &= \left(\delta(t) - m_{n_a}^{(n_a)}(t)\right) * y_0(t). \end{aligned} \quad (17)$$

In practice, we must consider the measurement $y(t)$ of the true output $y_0(t)$ in the above formulation. Therefore, let us define the output of the continuous-time LPV RPM-based model

$$y(t, \widehat{\boldsymbol{\theta}}^{RPM}) = \boldsymbol{\phi}^\top(t)\widehat{\boldsymbol{\theta}}^{RPM} + \gamma^y(t), \quad (18)$$

where $\boldsymbol{\phi}(t)$ is given by $\boldsymbol{\varphi}(t)$ defined in (15) by substituting $y_0(t)$ for $y(t)$, and

$$\begin{aligned} \widehat{\boldsymbol{\theta}}^{RPM} = [&\hat{a}_0^0, \dots, \hat{a}_0^{r_f}, \dots, \hat{a}_{n_a-1}^0, \dots, \hat{a}_{n_a-1}^{r_f}, \\ &\hat{b}_0^0, \dots, \hat{b}_0^{r_g}, \dots, \hat{b}_{n_b}^0, \dots, \hat{b}_{n_b}^{r_g}]^\top \end{aligned} \quad (19)$$

is the estimated parameter vector.

4.3. The parameter estimators

4.3.1. The least-squares estimate

Considering the measured data set $\{u(k\Delta t),\ y(k\Delta t),\ \rho(k\Delta t)\}_{k=0,\cdots,N_t}$, the least-squares estimate is given by

$$\begin{aligned} \widehat{\boldsymbol{\theta}}^{RPM} = [&\sum_{k=\widehat{\mathcal{T}}}^{N_t} \boldsymbol{\phi}(k\Delta t)\boldsymbol{\phi}^\top(k\Delta t)]^{-1} \\ &\sum_{k=\widehat{\mathcal{T}}}^{N_t} \boldsymbol{\phi}(k\Delta t)(y(k\Delta t) - \gamma^y(k\Delta t)), \end{aligned} \quad (20)$$

where $\widehat{T} = \widehat{\mathcal{T}}\Delta t$ is the design parameter, *i.e* the reinitialization parameter.

Details how to choose $\widehat{T}$ and to implement the RPM approach are given in (Ouvrard and Trigeassou, 2011; Ouvrard et al., 2024). The presence of the noisy output in the regresssor $\boldsymbol{\phi}(t)$ leads to a bias in the estimate $\widehat{\boldsymbol{\theta}}^{RPM}$. There are several ways to reduce the bias of the Least Squares estimation. To stay with an equation-error approach, the use of an instrumental variable reduces the bias. A second solution is to initialize an output error approach with the Least Squares estimate. In this work, we have opted for the output error approach. To demonstrate the relevance of this choice, we have carried out stochastic simulations comparing the results obtained by implementing an instrumental variable with those obtained with output error. Before presenting these results in Section 5, we recall the principle behind these two approaches.

4.3.2. The instrumental variable approach

The Instrumental Variable (IV) approach is widely applied to reduce estimation bias caused by measurement noise in system identification (Young, 1970; Söderström and Stoica, 1983), especially for LPV models estimation (Tóth et al., 2012). By introducing an auxiliary model that serves as an instrument, uncorrelated with noise yet correlated with the system's dynamic variables, the IV effectively reduces the effect of noise on parameter estimates (Ouvrard and Trigeassou, 2011; Ouvrard et al., 2024).

Therefore, to eliminate the bias on $\widehat{\boldsymbol{\theta}}^{RPM}$, we use an iterative IV approach initialized with the reinitialized partial moment-based model (RPM) estimate $\widehat{\boldsymbol{\theta}}^{RPM}$. In this process, we iteratively update an estimation vector, $\widehat{\boldsymbol{\theta}}^{IV}_{iter}$, starting from $\widehat{\boldsymbol{\theta}}^{IV}_{0} = \widehat{\boldsymbol{\theta}}^{RPM}$. At each iteration, we calculate an instrument denoted $\widehat{y}(t, \widehat{\boldsymbol{\theta}}^{IV}_{iter})$, which is independent of the noise $v(t)$ and derived from simulating the LPV system (Equation 3) using the parameter vector $\widehat{\boldsymbol{\theta}}^{IV}_{iter-1}$ obtained at the previous iteration and the following vector

$$\boldsymbol{\psi}(t) = \begin{bmatrix} \vdots \\ \displaystyle\sum_{k=0}^{i} (-1)^k \alpha_{i-k} \begin{pmatrix} i \\ k \end{pmatrix} \boldsymbol{F}^{(k)}\widehat{y}(t) \\ \vdots \\ \displaystyle\sum_{k=0}^{j} (-1)^k \beta_{j-k} \begin{pmatrix} j \\ k \end{pmatrix} \boldsymbol{G}^{(k)}u(t) \\ \vdots \end{bmatrix}. \tag{21}$$

A new parameter vector can be estimated as follows

$$\widehat{\boldsymbol{\theta}}^{IV}_{iter} = [\sum_{k=\widehat{\mathcal{T}}}^{N_t} \boldsymbol{\psi}(k\Delta t)\boldsymbol{\phi}^\top(k\Delta t)]^{-1} \sum_{k=\widehat{\mathcal{T}}}^{N_t} \boldsymbol{\psi}(k\Delta t)(y(k\Delta t) - \gamma^y(k\Delta t)). \tag{22}$$

This iterative procedure is repeated four or five times as recommended in (Ouvrard et al., 2024)).

4.3.3. An initialization for an output-error algorithm

The Levenberg-Marquardt algorithm (Nocedal and Wright, 2006) is an output-error algorithm which is asymptotically unbiased. The main difficulty is the possible convergence towards local minima of the criterion (6). Facing this problem, an alternative is to initialize the iterative procedure close to the optimal parameter vector.

Let us consider the Levenberg-Marquardt algorithm implemented as follows

$$\widehat{\boldsymbol{\theta}}^{OE}_{iter+1} = \widehat{\boldsymbol{\theta}}^{OE}_{iter} - \left\{ \left(\mathbf{J}''_{\theta\theta} + \mu \mathbf{I}_{N_\theta \times N_\theta}\right)^{-1} \mathbf{J}'_\theta \right\}_{\boldsymbol{\theta}=\widehat{\boldsymbol{\theta}}^{OE}_{iter}}, \tag{23}$$

with μ, a tuning parameter, $\mathbf{I}_{N_\theta \times N_\theta}$, an identity matrix, and the gradient and the pseudo-Hessian respectively defined by

$$\begin{aligned} \mathbf{J}'_\theta &= \frac{-2}{N_t+1} \sum_{k=0}^{N_t} (y(k\Delta t) - \widehat{y}(k\Delta t, \boldsymbol{\theta}))\boldsymbol{\sigma}(k\Delta t, \boldsymbol{\theta}), \\ \mathbf{J}''_{\theta\theta} &\approx \frac{2}{N_t+1} \sum_{k=0}^{N_t} \boldsymbol{\sigma}(k\Delta t, \boldsymbol{\theta})\boldsymbol{\sigma}^\top(k\Delta t, \boldsymbol{\theta}), \end{aligned} \tag{24}$$

where $\boldsymbol{\sigma}(t, \boldsymbol{\theta}) = \left[\ldots, \sigma_{a_j^\ell}(t), \ldots, \sigma_{b_j^\ell}(t), \ldots\right]^\top$ is the vector of the sensitivity functions deduced from $\frac{\partial \widehat{y}(t,\boldsymbol{\theta})}{\partial \boldsymbol{\theta}}$. The model output $\widehat{y}(t, \boldsymbol{\theta})$ is obtained by the simulation of (3) with the estimated parameter $\widehat{\boldsymbol{\theta}}^{OE}_{iter}$. The sensitivity functions are simulated similarly as follows

$$\sigma^{(n_a)}_{a_j^\ell}(t) = -\sum_{i=0}^{n_a-1} a_i(\rho)\sigma^{(i)}_{a_j^\ell}(t) - f_\ell(\rho)\widehat{y}^{(j)}(t, \boldsymbol{\theta}), \tag{25}$$

$$\sigma^{(n_a)}_{b_j^\ell}(t) = -\sum_{i=0}^{n_a-1} a_i(\rho)\sigma^{(i)}_{b_j^\ell}(t) + g_\ell(\rho)u^{(j)}(t), \tag{26}$$

with $f_0(\rho) = 1$ and $g_0(\rho) = 1$.

$\widehat{\boldsymbol{\theta}}^{RPM}$, obtained with equation (20), is a good initialization for $\widehat{\boldsymbol{\theta}}^{OE}_0$ of the iterative procedure (23).

5. Simulation example

Before applying the proposed approach to the nitrification process, we will first test it on a simplified numerical example with a system structure similar to that used in the nitrification model. The purpose of this example is to validate our algorithms within a framework that employs the same LPV model structure and parameter configuration as the nitrification process. This ensures that the equations and methods we use in the example are directly applicable to the nitrification process, demonstrating the relevance and effectiveness of the approach in real-world scenarios.

5.1. The true system

Consider a continuous-time SISO LPV system described as follows

$$y_0^{(1)}(t) = -a_0 y_0(t) + b_0 u(t) + b_1 u^{(1)}(t). \qquad (27)$$

Here, the coefficients depend on scheduling variables ρ_1, ρ_2, and ρ_3 through polynomial functions

$$\begin{aligned} a_0 &= 1 + 3\rho_1(t) + 2\rho_2(t) - \rho_3(t), \\ b_0 &= 1 - \rho_1(t) - 2\rho_2(t) - 0.5\rho_3(t), \\ b_1 &= 1 + \rho_1(t) + \rho_2(t) + 2\rho_3(t). \end{aligned} \qquad (28)$$

The continuous-time noise-free output $y_0(t)$ is sampled with a period of $\Delta t = 0.1s$ and a total length of $N_t = 1000$. The initial condition for $y_0(t)$ is $y_0(0) = -5.45$. A zero-mean white noise, denoted as $v(k\Delta t)$, added to the output samples, with a specified signal-to-noise ratio (SNR). The input signal is a pseudo-random binary sequence. The sequence was generated with pulse durations ranging from 5 to 30 sampling periods, alternating between two amplitude levels with -5 and 5. The noise-free scheduling signals are defined by

$$\begin{aligned} \rho_1(t) &= 0.3\sin(0.2t) - 0.01t - 0.01, \\ \rho_2(t) &= 0.03t - 0.1, \\ \rho_3(t) &= 0.2\sin(0.5t) - 0.01t + 0.1. \end{aligned} \qquad (29)$$

These signals along with the corresponding output $y_0(t)$ are visualized in Figure 2. The parameter variations are illustrated in Figure 3.

5.2. Monte Carlo simulation

A Monte Carlo simulation is executed to demonstrate the performance of the approach, comprising $n_{runs} = 100$ with the design parameter $\widehat{T} = 2\ s$. This design parameter is chosen in relation to the main time constant as presented in (Ouvrard et al., 2024). The simulation is carried out for three different SNR: 10 dB, 20 dB, and 30 dB. These SNR values are selected to represent high, medium, and low levels of noise, respectively, allowing us to evaluate the robustness of the proposed estimation method under various noise conditions.

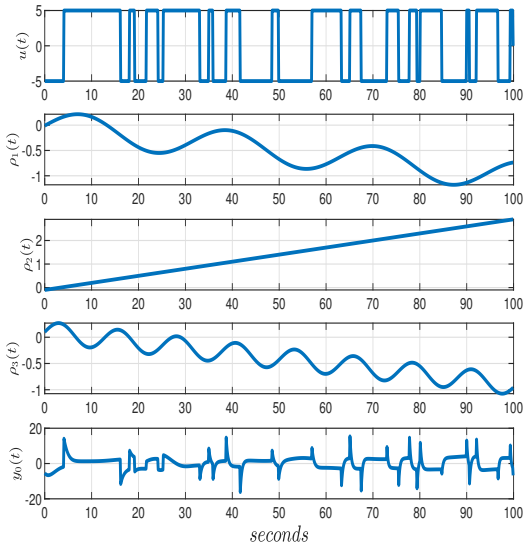

Figure 2: The simulated data set

We shall compare the three estimators outlined in Subsection 4.3 using the fitting percentage (FIT) and the normalized root mean square error ($RMSE$), which are defined as follows

$$FIT = 100 \times \left(1 - \frac{\|y_0(t) - \hat{y}(t)\|}{\|y_0(t) - mean(y_0(t))\|}\right) \qquad (30)$$

and

$$RMSE = \sqrt{\frac{1}{n_{runs}} \sum_{i=1}^{n_{runs}} \left(\frac{\theta_j^0 - \hat{\theta}_j(i)}{\theta_j^0}\right)^2}, \qquad (31)$$

with θ_j^0 the j-th parameter of $\boldsymbol{\theta}$ and $\hat{\theta}_j(i)$ the j-th parameter of $\widehat{\boldsymbol{\theta}}^{RPM}$ estimated with the i-th run.

Figure 4 illustrates a comparison between the true system output $y_0(t)$ and the outputs generated by three different parametric estimation methods: RPM, IV and OE. This comparison is based on a single realization out of 100 Monte Carlo runs for different SNR values. The OE method consistently shows the highest fit percentage (98.16%, 97.5%, and 96.04% for 30 dB, 20 dB, and 10 dB, respectively), followed by the IV method, which achieves 94.2%, 93%, and 92.17% across the same SNR levels. RPM ranks slightly lower with fit percentages of 92.9%, 91.4%, and 89.94%. In error analy-

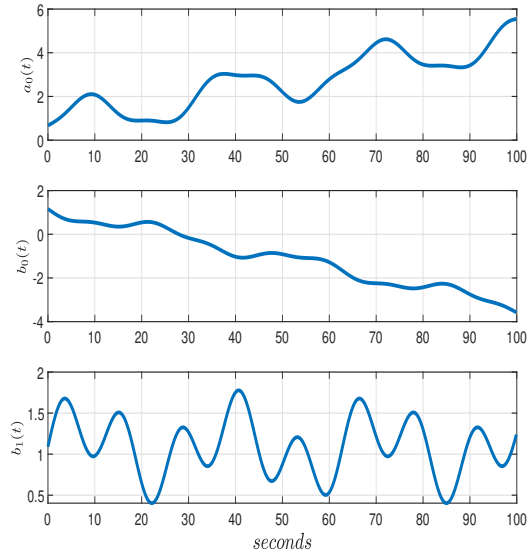

Figure 3: The parameter variations with $\rho_1(t)$, $\rho_2(t)$ and $\rho_3(t)$

sis, OE demonstrates the lowest error variance, indicating strong robustness to noise. The IV method shows moderate error variance, compared to RPM, that shows the largest error spread, suggesting greater sensitivity to noise.

The results of the Monte Carlo study are presented in Figures 5 to 7 and Tables 1 to 4 for various signal-to-noise ratios. When the noise level is low (refer to Figure 5 and Table 1), the least-squares estimates $\widehat{\boldsymbol{\theta}}^{RPM}$ are good. However, with a high noise level (refer to Figure 7 and Table 3), a significant bias is observed in the least-squares estimates $\widehat{\boldsymbol{\theta}}^{RPM}$. This bias can be reduced by either employing IV techniques or initializing the output-error algorithm. While the IV approach provides reliable estimates under different noise conditions, the OE algorithm demonstrated superior convergence properties and overall accuracy in identifying the LPV model parameters.

This study shows that an identification strategy coupling reinitialized partial moments and the Levenberg-Marquardt algorithm yields best estimates. After thorough validation of the proposed methodology using Monte Carlo simulation, this strategy will be applied in the next section to a practical nitrification process.

6. Application to the nitrification process: A case study

Let us consider the parametric estimation of an LPV model using the Levenberg-Marquardt algorithm to represent the nitrification process described in Subsection 2.4.

6.1. LPV model structure of the process

To evaluate the economical and environmental impacts of their processes, the SIAAP has developed a simulation software named SimBio to represent the Seine Aval biofiltration processes (Bernier et al., 2014; Rocher et al., 2014a,b). Based on this simulator, a preliminary study was carried out to analyze the process nonlinearities and to select an appropriate LPV model structure (Boutourda et al., 2024). Thus, multiple simulations have been conducted using small magnitudes of Q_{air} for various operating points. Figure 8 shows one example of simulation for one operating point: C_{in} = 22 mgN/L, $Q_{water} = 3 * 10^4$ m^3/d and Q_{air} varying around $7 * 10^4$ Nm^3/d (Note that the oscillations visible in the quasi-permanent regimes of C_{out} are linked to the daily washing of the biofilters). These experiments have revealed two distinct dynamics that we aim to capture within the LPV model framework: a fast dynamic (lasting a few minutes), which can be adequately modeled with a direct transfer function and a delay of one sampling time between Q_{air} and C_{out}, and a slow dynamic (spanning a few days). Therefore, we have opted for the following LPV model structure :

$$\frac{C_{out}(s)}{Q_{air}(s)} = (K_0 + \frac{K_1}{1+\tau s})e^{-\Delta t s} = \frac{b_0 + b_1 s}{a_0 + s}e^{-\Delta t s}, \quad (32)$$

with parameters b_0, b_1 and a_0 depending on scheduling variables Q_{air}, Q_{water} and C_{in}. This LPV model is a behavioral model and the parameters K_0, K_1, τ, a_0, a_1 and b_1 used in the model do not have a direct physical significance.

Various polynomial orders have been examined for the varying parameters and compared in terms of fitting percentage. Hence, a first order was selected, which represents a good compromise between model complexity and model response accuracy. Then, a_0, b_0 and b_1 are defined as follows

$$\begin{aligned} a_0 &= a_0^0 + a_0^1 Q_{air} + a_0^2 Q_{water} + a_0^3 C_{in}, \\ b_0 &= b_0^0 + b_0^1 Q_{air} + b_0^2 Q_{water} + b_0^3 C_{in}, \\ b_1 &= b_1^0 + b_1^1 Q_{air} + b_1^2 Q_{water} + b_1^3 C_{in}. \end{aligned} \quad (33)$$

6.2. Real data set

The signals Q_{air}, Q_{water}, C_{in} and C_{out} are measured data from the Seine Aval wastewater treatment plant. These measurements were obtained with a sampling time period of 15 minutes throughout the winter season of 2019 for 50 days.

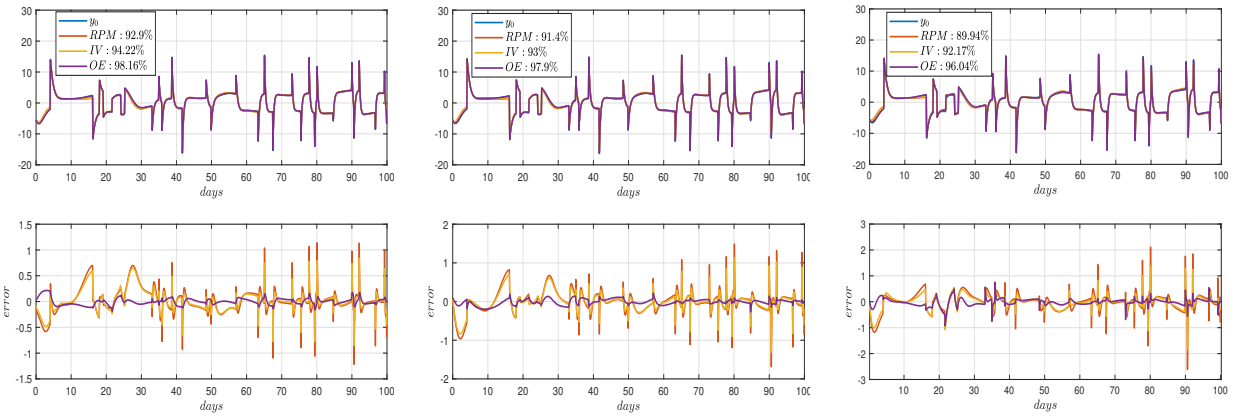

(a) $SNR = 30dB$ (b) $SNR = 20dB$ (c) $SNR = 10dB$

Figure 4: Comparison of the system output $y_0(t)$ and estimated outputs from RPM, IV, and OE methods

Table 1: Estimates with Monte Carlo simulations and $SNR = 30dB$

		$\widehat{\boldsymbol{\theta}}^{RPM}$			$\widehat{\boldsymbol{\theta}}^{IV}$			$\widehat{\boldsymbol{\theta}}^{OE}$		
	True	Mean	Std	RMSE	Mean	Std	RMSE	Mean	Std	RMSE
a_0^0	1	0.896	0.058	0.119	0.936	0.057	0.086	1.01	0.053	0.054
a_0^1	3	2.593	0.121	0.141	2.714	0.123	0.104	3.004	0.121	0.04
a_0^2	2	1.812	0.082	0.102	1.865	0.086	0.08	1.993	0.084	0.042
a_0^3	-1	-0.603	0.17	0.432	-0.703	0.172	0.343	-1.018	0.181	0.181
b_0^0	1	0.826	0.028	0.177	0.859	0.029	0.144	1.004	0.023	0.023
b_0^1	-1	-0.87	0.056	0.142	-0.888	0.058	0.126	-1.006	0.058	0.058
b_0^2	-2	-1.847	0.052	0.081	-1.89	0.053	0.061	-2.009	0.048	0.024
b_0^3	-0.5	-0.737	0.083	0.502	-0.707	0.086	0.449	-0.516	0.081	0.164
b_1^0	1	0.999	0.025	0.025	1.01	0.025	0.027	1.002	0.022	0.022
b_1^1	1	0.9	0.064	0.119	0.954	0.065	0.079	1.004	0.051	0.051
b_1^2	1	0.852	0.031	0.152	0.89	0.031	0.114	1.003	0.029	0.029
b_1^3	2	1.845	0.079	0.087	1.864	0.082	0.079	2.003	0.078	0.039

Table 2: Estimates with Monte Carlo simulations and $SNR = 20dB$

		$\widehat{\boldsymbol{\theta}}^{RPM}$			$\widehat{\boldsymbol{\theta}}^{IV}$			$\widehat{\boldsymbol{\theta}}^{OE}$		
	True	Mean	Std	RMSE	Mean	Std	RMSE	Mean	Std	RMSE
a_0^0	1	0.866	0.058	0.146	0.921	0.059	0.099	0.995	0.061	0.061
a_0^1	3	2.516	0.155	0.169	2.677	0.163	0.12	2.967	0.15	0.051
a_0^2	2	1.793	0.088	0.112	1.866	0.093	0.082	1.989	0.096	0.048
a_0^3	-1	-0.529	0.199	0.511	-0.658	0.203	0.397	-0.982	0.219	0.218
b_0^0	1	0.802	0.034	0.2	0.848	0.036	0.156	0.991	0.036	0.037
b_0^1	-1	-0.854	0.064	0.159	-0.878	0.066	0.139	-0.996	0.067	0.067
b_0^2	-2	-1.813	0.058	0.098	-1.87	0.06	0.072	-1.988	0.06	0.03
b_0^3	-0.5	-0.724	0.087	0.48	-0.683	0.092	0.409	-0.496	0.089	0.177
b_1^0	1	0.994	0.028	0.029	1.009	0.029	0.03	0.999	0.026	0.026
b_1^1	1	0.874	0.081	0.15	0.947	0.084	0.099	0.991	0.068	0.068
b_1^2	1	0.831	0.041	0.174	0.884	0.041	0.123	0.996	0.036	0.036
b_1^3	2	1.829	0.109	0.101	1.856	0.113	0.091	2.001	0.107	0.053

Table 3: Estimates with Monte Carlo simulations and $SNR = 10dB$

		$\widehat{\boldsymbol{\theta}}^{RPM}$			$\widehat{\boldsymbol{\theta}}^{IV}$			$\widehat{\boldsymbol{\theta}}^{OE}$		
	True	Mean	Std	RMSE	Mean	Std	RMSE	Mean	Std	RMSE
a_0^0	1	0.829	0.088	0.192	0.938	0.092	0.111	1.01	0.088	0.088
a_0^1	3	2.393	0.186	0.212	2.706	0.199	0.118	3.002	0.179	0.06
a_0^2	2	1.734	0.151	0.153	1.872	0.169	0.106	2.007	0.159	0.079
a_0^3	-1	-0.42	0.299	0.652	-0.661	0.337	0.477	-0.979	0.342	0.341
b_0^0	1	0.77	0.047	0.235	0.857	0.05	0.151	1.001	0.044	0.044
b_0^1	-1	-0.832	0.087	0.189	-0.879	0.095	0.154	-0.986	0.101	0.101
b_0^2	-2	-1.763	0.074	0.124	-1.871	0.079	0.076	-1.988	0.08	0.04
b_0^3	-0.5	-0.732	0.122	0.524	-0.652	0.137	0.408	-0.464	0.127	0.262
b_1^0	1	0.98	0.035	0.041	1.009	0.036	0.037	1.002	0.033	0.033
b_1^1	1	0.798	0.101	0.225	0.938	0.107	0.123	1.008	0.087	0.086
b_1^2	1	0.787	0.054	0.22	0.887	0.056	0.126	1.004	0.057	0.057
b_1^3	2	1.822	0.144	0.114	1.875	0.159	0.101	2.002	0.163	0.081

Table 4: *FIT (%) vs. SNR*

	$SNR = 30dB$			$SNR = 20dB$			$SNR = 10dB$		
	Min	Mean	Max	Min	Mean	Max	Min	Mean	Max
$\widehat{\boldsymbol{\theta}}^{RPM}$	89.89	91.51	93.26	88.77	90.71	92.44	85.97	88.82	91.78
$\widehat{\boldsymbol{\theta}}^{IV}$	91.21	92.77	94.48	90.52	92.43	94.24	89.51	92.09	94.75
$\widehat{\boldsymbol{\theta}}^{OE}$	97.03	97.95	98.82	96.16	97.38	98.56	94.41	96.41	97.81

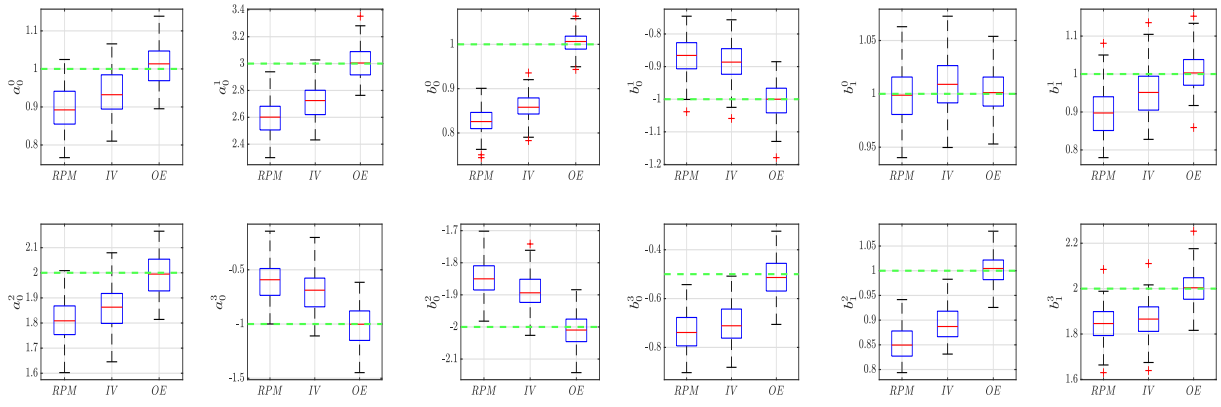

(a) a_0 (b) b_0 (c) b_1

Figure 5: Box plots of parameters estimation for $SNR = 30dB$

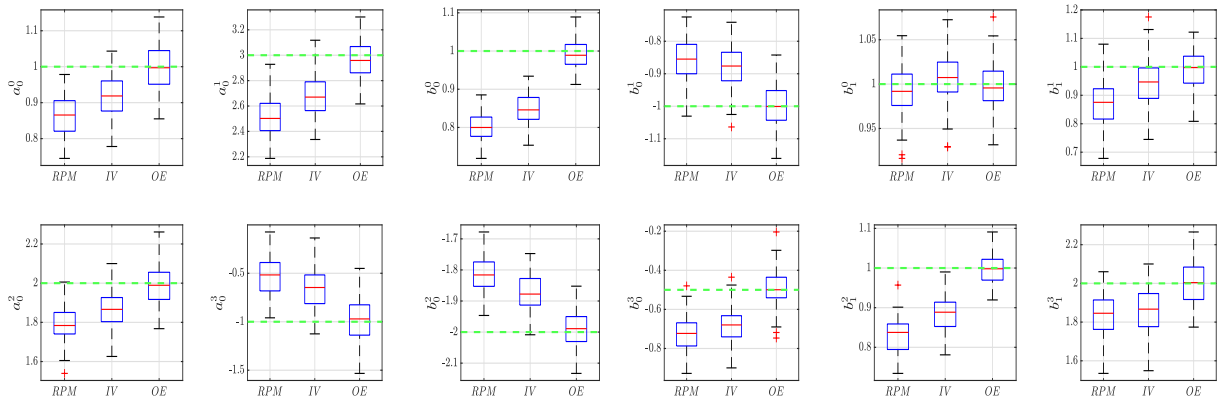

(a) a_0 (b) b_0 (c) b_1

Figure 6: Box plots of parameters estimation for $SNR = 20dB$

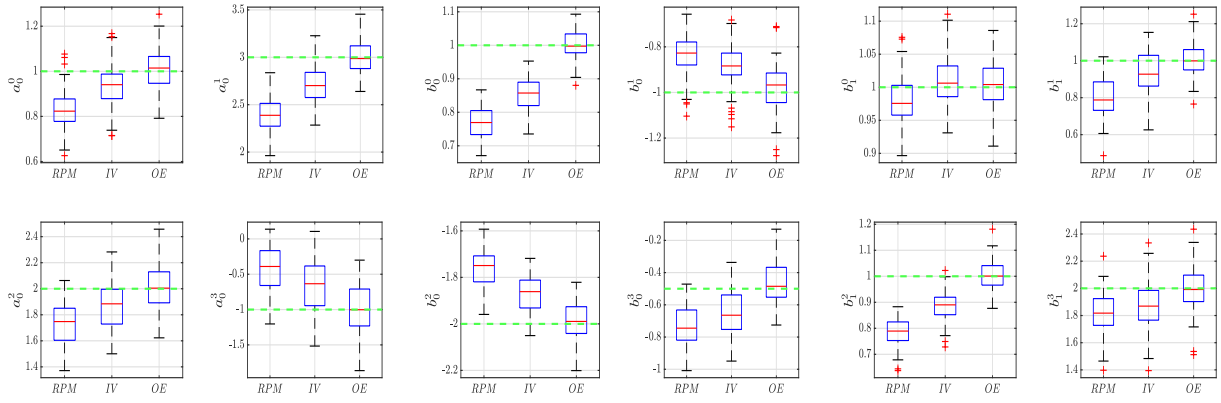

(a) a_0 (b) b_0 (c) b_1

Figure 7: Box plots of parameters estimation for $SNR = 10dB$

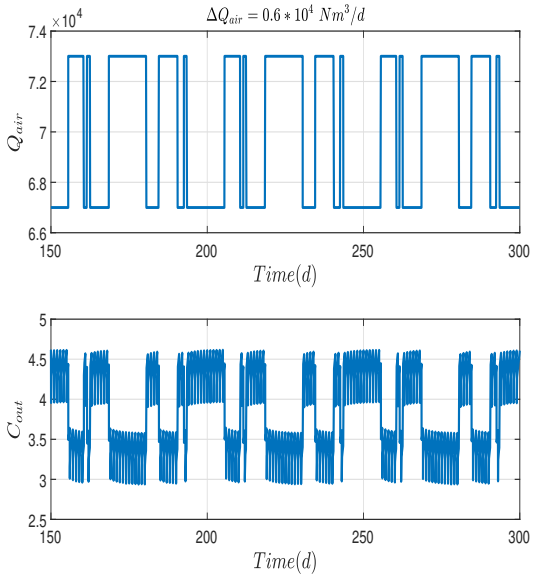

Figure 8: Selected input Q_{air} and output C_{out} generated by SimBio simulator for $C_{in} = 22\ mgN/L$ and $Q_{water} = 3 * 10^4\ m^3/d$

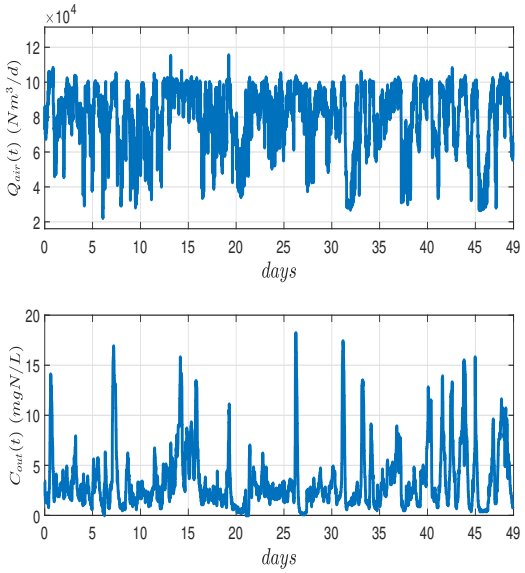

Figure 9: Input Q_{air} and output C_{out} of the nitrification process

During this period, the ammonium concentration C_{in} fluctuated between a low value of 5.9 mgN/L and a high value of 35.7 mgN/L. For Q_{water}, the variation range spanned from 1.01e4 m^3/d to 5.8e4 m^3/d, while Q_{air} varied between 2.21e4 Nm^3/d and 1.15e5 Nm^3/d . This variability ensures that the signals are sufficiently rich to cover the operating range. It is important to note that Q_{water} and Q_{air} values represent the variation for one biofilter.

Figure 9 illustrates both the input and the output of the nitrification system Q_{air} and C_{out}, while Figure 10 displays the scheduling variables Q_{air}, Q_{water} and C_{in}.

6.3. *Parametric estimation and validation*

In order to identify the 12 parameters in (33), we must first use the LPV RPM-based model method, as detailed in Subsection 4.2.

Considering C_{out} and Q_{air}, the vector $\boldsymbol{\phi(t)}$ in Eq. (18) will be expressed as follows

$$\boldsymbol{\phi}(t) = \begin{bmatrix} \alpha_0^{\boldsymbol{F}(t)C_{out}(t)}(t) \\ \beta_0^{\boldsymbol{G}(t)Q_{air}(t-1)}(t) \\ \beta_1^{\boldsymbol{G}(t)Q_{air}(t-1)}(t) - \beta_0^{\boldsymbol{G}^{(1)}(t)Q_{air}(t-1)}(t) \end{bmatrix} \quad (34)$$

with $\boldsymbol{F}(t) = \boldsymbol{G}(t) = \begin{bmatrix} 1 & Q_{air}(t) & Q_{water}(t) & C_{in}(t) \end{bmatrix}^T$.

An identification study was conducted using one set of data and a validation test with another one corresponding to the same conditions. The initial 25 days of collected data (Figures 9-10) were used for parametric estimation and the last 25 days were reserved for the purpose of validating the LPV model.

The fitting percentage (calculated by (30)) between the LPV RPM-based model output and the identification data output is 36.16 %. For the validation data, the fitting percentage is 32.9%.

From the LPV RPM-based model, we have initialized the parameter vector $\widehat{\boldsymbol{\theta}}_0^{OE}$ in (23) to achieve an optimum parameter vector. Following the parameter initialization, the Levenberg-Marquardt algorithm is executed, using the equations outlined in Subsection 4.3.3. It required six iterations to converge. The estimated parameter values are presented in Table 5. The variations of final parameters estimated with OE approach are shown in Figure 11.

Figure 12 illustrates the identification results. C_{out} represents the system output, whereas $\hat{C}_{out}$ is the output generated by the LPV model with $\widehat{\boldsymbol{\theta}}_6^{OE}$. A fitting percentage of 55.58% is observed between the two signals. As highlighted by (Muroi and Adachi, 2015), the fitting ratio can be sensitive to high-amplitude systems, often resulting in lower FIT values compared to low-amplitude cases. Considering the complexity of the nitrification process and the wide range operating conditions, the FIT percentage between the two signals is acceptable for this application. The model faithfully re-

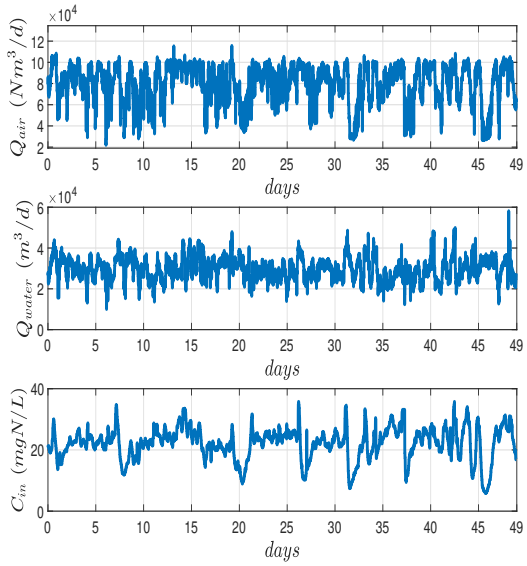

Figure 10: Measured scheduling variables Q_{air}, Q_{water} and C_{in}

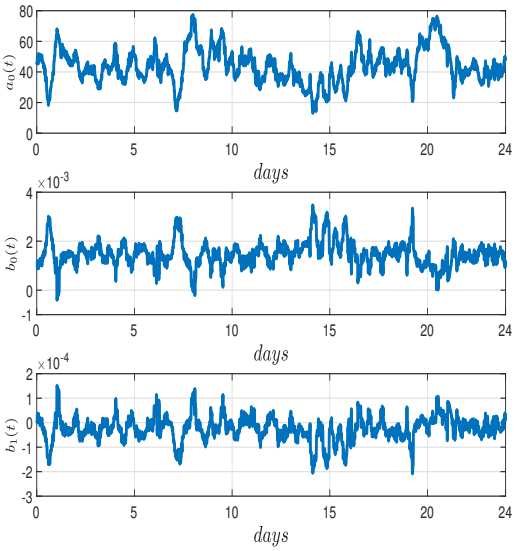

Figure 11: Estimated parameter variations with $Q_{air}(t)$, $Q_{water}(t)$ and $C_{in}(t)$

produces the behaviour of the nitrification process. Figure 13 shows a comparison between the measured output, the LPV RPM-based model output and the considered LPV model output.

The next step is to use the second set of data to validate the model. Validation results are presented in Figure 14. With a fitting percentage of 49.35% during validation, we can confidently assert that the LPV model reasonably represents the complex dynamics of the nitrification process.

7. Conclusion

This work has introduced a novel methodology for estimating LPV model parameters, based on the reinitialized partial moment method within a global identification framework. A continuous-time LPV reinitialized partial moment-based model was proposed, and key parameter estimation techniques, such as the least-squares estimate, instrumental variable approach, and the output-error algorithm, specifically the Levenberg-Marquardt algorithm, were employed.

The results from the Monte Carlo simulations demonstrate the robustness of the proposed LPV modeling approach. The simulations effectively provide accurate parameter estimates and system responses. They further underscore the impact of the signal-to-noise ratio on estimation accuracy, with increased standard deviation and root mean square error, and decreased fitting percentage observed at lower SNR levels. Despite the noise, all estimates obtained using the reinitialized partial moment (RPM) approach served as reliable initializations for the subsequent iterative procedures. The Levenberg-Marquardt algorithm, in particular, demonstrated superior performance in identifying LPV model parameters compared to the instrumental variable (IV) method, showing greater resilience under varying noise conditions.

The results were promising, which allows us to apply this methodology to the real-world problem of nitrification in wastewater treatment.The developed continuous-time LPV model successfully captured the complex dynamics of the biological nitrification process, offering a valuable tool for understanding and controlling ammonia removal. The model's ability to adapt to varying operating conditions demonstrates its practical utility for optimizing nitrification processes in wastewater treatment plants. This optimization is envisaged in future work.

Acknowledgements

This work benefits from the financial support of the research program *MOCOPÉE* (an acronym of the French words "MOdélisation, Contrôle et Optimisation des Procédés d'Épuration des Eaux") and of the Cadi Ayyad University.

Table 5: Estimated parameter values for using RPM (first line of values) and OE (second line of values)

a_0				b_0				b_1			
a_0^0	a_0^1	a_0^2	a_0^3	b_0^0	b_0^1	b_0^2	b_0^3	b_1^0	b_1^1	b_1^2	b_1^3
6.14	2e-04	-2.48e-04	-0.43	-9.22e-04	5.41e-10	1.67e-08	2.53e-05	-2.3e-05	3.67e-10	-5.58e-10	2.13e-06
113.47	-1.7e-04	-4.53e-04	-1.93	-2.3e-03	-9.26e-09	7.89e-08	9.9e-05	3.36e-04	6.53e-10	-8.32e-09	-7.38e-06

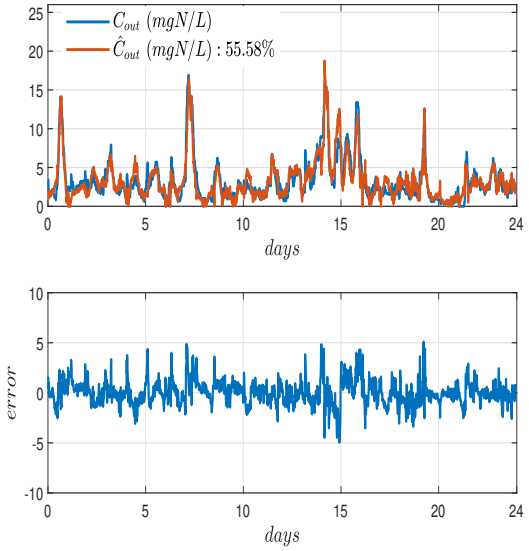

Figure 12: Identification output data C_{out} and simulated LPV model output $\hat{C}_{out}$

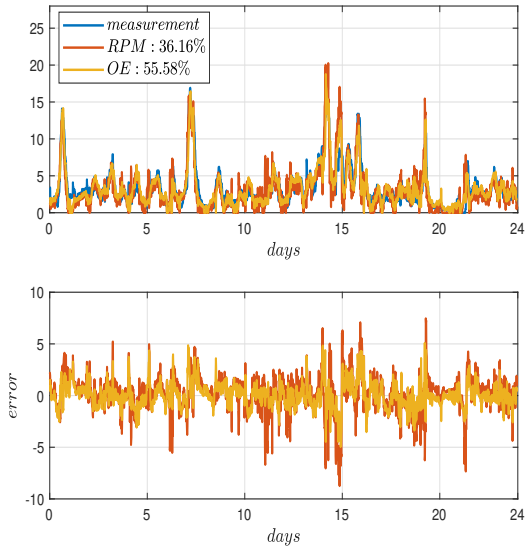

Figure 13: Comparison between the system output, LPV-RPM model and the final model estimated with the OE approach

References

Bamieh, B., Giarré, L., 2002. Identification of linear parameter varying models. International Journal of Robust and Nonlinear Control 12, 841–853.

Bernier, J., Rocher, V., Guerin, S., Lessard, P., 2014. Modelling the nitrification in a full-scale tertiary biological aerated filter unit. Bioprocess and Biosystems Engineering 37, 289–300.

Boutourda, F.Z., Ouvrard, R., Poinot, T., Mehdi, D., Mesquine, F., De Tredern, E., Jauzein, V., 2024. A global approach to estimate continuous-time LPV models for wastewater nitrification, in: 20th IFAC Symposium on System Identification Conference, Boston, USA, 61-66.

Canler, J.P., Perret, J.M., Lengrand, F., Iwema, A., 2003. Nitrification in biofilters under variable load and low temperature. Water Science and Technology 47 (11), 129–136.

Chouaba, S., Chamroo, A., Ouvrard, R., Poinot, T., 2011. Continuous-time identification of linear parameter varying model using an output-error technique, in: IFAC World Congress.

De Caigny, J., Camino, J., Swevers, J., 2009. Interpolating model identification for SISO linear parameter-varying systems. Mechanical Systems and Signal Processing 23, 2395–2417.

Felici, F., van Wingerden, J., Verhaegen, M., 2007. Subspace identification of MIMO LPV systems using periodic scheduling sequence. Automatica 43, 1684–1697.

Giarré, L., Bauso, D., Falugi, P., Bamieh, B., 2006. LPV model identification for gain scheduling control: an application to rotating stal and surge control problem. Control Engineering Practice 14, 351–361.

Henze, M., Grady, C.P.L., Gujer, W., v. R. Marais, G., Matsuo, T., 1987. Activated sludge model no. 1. IAWPRC Scientific and Technical Report No. 1 .

Henze, M., van Loosdrecht, M., Ekama, G., Brdjanovic, D., 2008. Biological wastewater treatment: Principles, modelling and design. IWA Publishing, United Kingdom.

Laurain, V., Gilson, M., Toth, R., Garnier, H., 2010. Refined instrumental variable methods for identification of LPV Box-Jenkins models. Automatica 46, 959–967.

Laurain, V., Toth, R., Gilson, M., Garnier, H., 2011. Direct identification of continuous-time linear parameter-varying input/output models. IET Control Theory and Applications 5 (7), 878–888. doi:10.1049/iet-cta.2010.0218.

Lee, L., Poolla, K., 1999. Identification of linear parameter varying systems using non linear programming. Journal of Dynamic Systems, Measurements and Control 121, 71–78.

Lovera, M., Mercère, G., 2007. Identification for gain scheduling: a balanced subspace approach, in: Proceedings of the 26th American Control Conference, New York, USA.

Mendoza-Espinosa, L., Stephenson, T., 1999. A review of biological aerated filters (bafs) for wastewater treatment. Environmental Engineering Science 16 (3), 201–216.

Mercère, G., Palsson, H., Poinot, T., 2011. Continuous-time linear parameter-varying identification of a cross flow heat exchanger: a local approach. IEEE Transactions on Control Systems Technology 19 (1), 64–76.

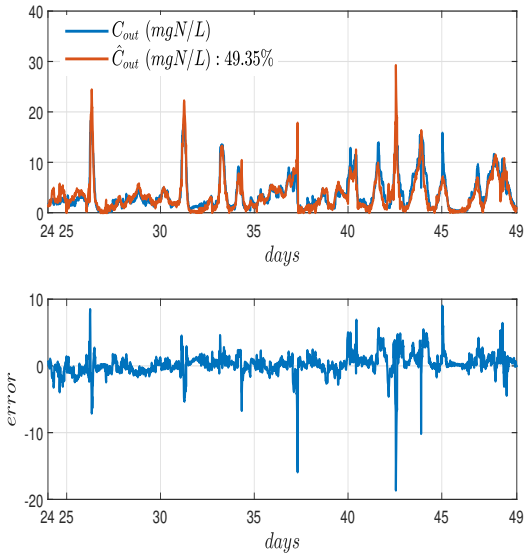

Figure 14: Validation output data C_{out} and simulated LPV model output $\hat{C}_{out}$

Metcalf & Eddy, I., Tchobanoglous, G., Burton, F., Stensel, H., 2003. Wastewater Engineering: Treatment and Reuse. McGraw-Hill higher education, McGraw-Hill Education.

Metcalf & Eddy, I., Tchobanoglous, G., Stensel, H.D., Tsuchihashi, R., Burton, F.L., 2014. Wastewater Engineering: Treatment and Resource Recovery. 5th ed., McGraw-Hill Education, New York.

Muroi, H., Adachi, S., 2015. Model validation criteria for system identification in time domain. IFAC-PapersOnLine 48, 86–91. doi:10.1016/j.ifacol.2015.12.105.

Nocedal, J., Wright, S., 2006. Numerical optimization. Springer-Verlag.

Ouvrard, R., Poinot, T., Trigeassou, J.C., 2024. Partial moments in system identification. Lecture Notes in Control and Information Sciences. Springer Cham.

Ouvrard, R., Trigeassou, J.C., 2011. On embedded FIR filter models for identifying continuous-time and discrete-time transfer functions: the RPM approach. International Journal of Control 84(3), 616–632.

Payraudeau, M., Paffoni, C., Gousailles, M., 2000. Tertiary nitrification in an up flow biofilter on floating media: influence of temperature and cod load. Water Science and Technology 41 (4-5), 21–27.

Pujol, R., Canler, J.P., Iwema, A., 1992. Biological aerated filters: An attractive and alternative biological process. Water Science Technology 26 (3-4), 693–702.

Rich, L.G., 1961. textsunit operations of sanitary engineering. John Wiley Sons, NewYork, États-Unis. .

Rocher, V., Bernier, J., Guerin, S., Lessard, P., 2014a. Modélisation du fonctionnement des biofiltres nitrifiants de la station d'épuration seine aval (SIAAP). 1. cas de l'encrassement et des pertes de charge. TSM 11, 106–118.

Rocher, V., Bernier, J., Guerin, S., Lessard, P., 2014b. Modélisation du fonctionnement des biofiltres nitrifiants de la station d'épuration seine aval (SIAAP). 1. cas des performances épuratoires. TSM 11, 85–102.

Rocher, V., Paffoni, C., Gonçalves, A., AZIMI, S., Gousailles, M., 2008. Municipal wastewater treatment by biofiltration: Siaap feedback. Journal of Water Science 21 (4), 475–485.

Steinbuch, M., van de Molengraft, R., van der Voort, A., 2003. Experimental modelling and LPV control of a motion system, in: Proceedings of the American Control Conference, Denver, Colorado, USA.

Stensel, H.D., Brenner, R.C., Lee, K.M., Melcer, H., Rakness, K., 1988. Biological aerated filter evaluation. Journal of Environmental Engineering 114 (3), 655–671.

Stensel, H.D., Reiber, S., 1983. Industrial wastewater treatment with a new biological fixed-film system. Environmental Progress 2 (2), 110–115.

Söderström, T., Stoica, P., 1983. Instrumental variable methods for system identification. Springer-Verlag, Berlin.

Toth, R., 2008. Modeling and identification of linear parameter-varying systems: an orthonormal basis function approach. Ph.D. thesis. Delft University of Technology. Delft, The Netherlands.

Toth, R., 2010. Modeling and identification of linear parameter-varying systems. Lecture Notes in Control and Information Sciences, Springer.

Tóth, R., Laurain, V., Gilson, M., Garnier, H., 2012. Instrumental variable scheme for closed-loop LPV model identification. Automatica 48, 2314–2320. doi:https://doi.org/10.1016/j.automatica.2012.06.037.

van Wingerden, J., Felici, F., Verhaegen, M., 2007. Subspace identification of MIMO LPV systems using piecewise constant scheduling sequence with hard/soft switching, in: Proceedings of the European Control Conference, Kos, Greece.

Verdult, V., Verhaegen, M., 2005. Kernel methods for subspace identification of multivariable LPV and bilinear systems. Automatica 41, 1557–1565.

Wei, X., Del Re, L., 2006. On persistent excitation for parameter estimation of quasi-LPV systems and its application in modeling of diesel engine torque, in: 14th IFAC Symposium on System Identification, Newcastle, Australia.

Young, P., 1970. An instrumental variable for real-time identification of a noisy process. Automatica 6, 271–287.

Zhu, J., 2020. Modélisation détaillée du fonctionnement de la future filière complète de biofiltration de la station de traitement des eaux usées Seine Aval. Ph.D. thesis. Université de Technologie de Compiègne.